World Electric Vehicle Journal

MDPI

Article

Proposed Model of Sustainable Resource Management for Smart Grid Utilization

Haider Ali Tauqeer [1,*], Faisal Saeed [1,*], Muhammad Hassan Yousuf [2], Haroon Ahmed [3], Asad Idrees [1], Muhammad Haseeb Khan [1] and Hasan Ertaza Gelani [4]

[1] Department of Electrical Engineering, SBASSE, Lahore University of Management Sciences (LUMS), Lahore 54792, Punjab, Pakistan; 19060046@lums.edu.pk (A.I.); 19060050@lums.edu.pk (M.H.K.)
[2] Department of Electrical Engineering, University of Engineering and Technology (UET) Lahore, Lahore 54890, Punjab, Pakistan; 2020msee137@student.uet.edu.pk
[3] Department of Electrical Engineering, Technische Universität (TU) Dortmund, North Rhine-Westphalia, 44227 Dortmund, Germany; haroon.ahmed@tu-dortmund.de
[4] Department of Electrical Engineering, University of Engineering and Technology (UET) Lahore, Faisalabad Campus, Faisalabad 38000, Punjab, Pakistan; erteza.gelani@uet.edu.pk
* Correspondence: 19060036@lums.edu.pk (H.A.T.); 19060005@lums.edu.pk (F.S.)

Abstract: Automation and modernization of the grid with the availability of micro-grids including non-conventional sources of energy are the main constituent of smart grid technology. Most energy demand is fulfilled by fossil fuel-based power plants. Inadequacy of fuel resources, higher operating costs, and ever-increasing carbon emissions are the primary constraints of fossil fuels-operated power plants. Sustainable energy resource utilization in meeting energy demand is thought to be a preferred solution for reducing carbon emissions and is also a sustainable economic solution. This research effort discusses an accurate mathematical modeling and simulation implementation of a sustainable energy resource model powered by solar, grid, and proton exchange membrane fuel cell (PEMFC) stack and focuses on the energy management of the model. In the proposed model, despite energy resources being sustainable, consumer side sustainability is achieved by using electrical charging vehicles (ECVs) to be integrated with sustainable resources. The proposed energy resource management (ERM) strategy is evaluated by simulating different operating conditions with and without distributed energy resources exhibiting the effectiveness of the proposed model. PEMFC is incorporated in the model to control fluctuations that have been synchronized with other energy resources for the distribution feeder line. In this proposed model, PEMFC is synchronized with grid and solar energy sources for both DC and AC load with ERM of all sources, making the system effective and reliable for consumer-based load and ECVs utilization.

Keywords: proton exchange membrane fuel cell; electrical charging vehicles; energy resource management

Citation: Tauqeer, H.A.; Saeed, F.; Yousuf, M.H.; Ahmed, H.; Idrees, A.; Khan, M.H.; Gelani, H.E. Proposed Model of Sustainable Resource Management for Smart Grid Utilization. *World Electr. Veh. J.* **2021**, *12*, 70. https://doi.org/10.3390/wevj12020070

Academic Editor: Joeri Van Mierlo

Received: 31 December 2020
Accepted: 26 April 2021
Published: 28 April 2021

1. Introduction

The intelligent grid has a controlled and communicated mechanism for the efficient energy flow within the power system, but the present demand is to make the grid smart by employing sustainable energy resources i.e., distributed and renewable energy resources (RERs). Most energy is fulfilled by coal-operated power plants whose operating cost is higher than RERs and the carbon emissions cause a bad air quality index (AQI). Advancement towards distributed energy resources (DERs) for power generation has been accounted as a better alternative power generation solution to reduce carbon emissions [1]. According to [2] solar energy has a carbon dioxide emission factor of 0.5Ton/MWh and hydro energy has an emission factor of 0.47 Ton/MWh which is much less than the coal emission factor per megawatt-hour (MWh). Economically and socially, a photovoltaic (PV) system is best suited as it overcomes carbon dioxide (CO_2) emissions while having a good payback period [3].

According to the live AQI forecast, considering the present, i.e., 2020 situation of Pakistan, there are many cities whose AQI is greater than 100 and that is hazardous per United States metrics and is shown in Figure 1. So sustainable environment implementation in the future accounting for all the RERs and the electrical vehicles (EVs), which are currently 46.2 percent fuel of Pakistan according to [4] and can aid in overcoming the energy supply and demand gap as well as fairly reduce the carbon emissions. Almost the same situation is prevailing in other regions of the world.

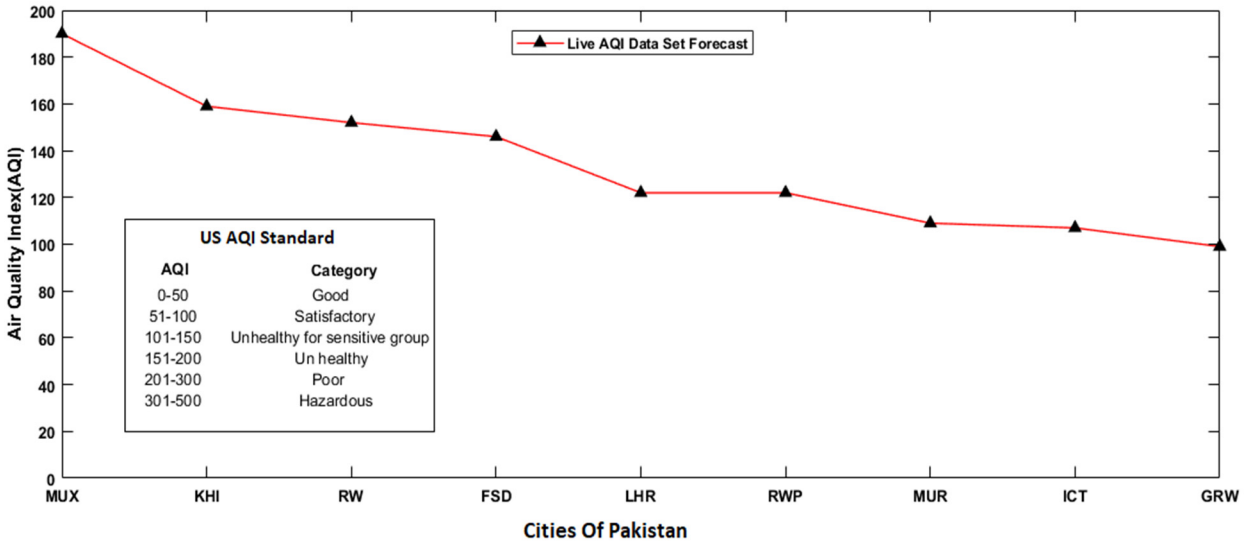

Figure 1. Live Air Quality Index forecast of Pakistan.

Now there is a need to automate the system to overcome the ramp rate by utilizing renewable energy sources i.e., solar, fuel cells, and wind, controlled by auto-recloser. Storage batteries are useful to store excess energy which overcomes the duck curve and use that energy in ECVs modules [5]. Smart and micro-grid systems lessen the need for a long high-voltage direct current (HVDC) transmission line as power demand can be consumed by DERs [6]. If the interconnected system has ramp response resources with non-conventional resources, then this distributed energy system can be utilized during peak hours [6,7]. Non-conventional power resource availability depends on atmospheric conditions, so planning and its efficiency calculation can be done with simulation tools like PVsyst for a solar system.

Power electronics for smart grids provide lossless switching for bulk energy storage and conversion of power per utilization and a recent advancement is its usage in EVs, HVDC transmission, and PV system [8–10]. For multi-voltage conversion, multilevel converters can be used which overcome the flexibility barrier of a specific grid. The cascaded bridge converters, also called modular multilevel converter, which have multiple configurations including single, double, and triple bridge cell, which is implementable in EVs' charging module as proposed by us. Multilevel converters can be used to control direct current (DC) voltages and control power losses [11]. For the interfacing of micro-grid with the DC line, thyristor line converters and IGBT-based voltage source converters are used for power control, which can lead to system stability. As the fuel cell is also part of distributed energy sources but its reliability has been increased by using a DC-DC boost converter for interfacing with the power system. Cascaded network for fuel cells comprises of DC-to-DC converter with inverter for rectification. High-frequency DC to AC converter is used in fuel cells to gain high power conversion by cyclo-converters [12,13]. For the PV system, a boost converter is used having a filter, with the inverter that controls the output power with boosting input voltage. Aggregation of different renewables sources into a single inverter is done by a single-ended primary inductance converter. The distribution

system used for the inverter should be resilient to enable the bidirectional flow of energy for DERs [14–16]. A challenge is to design the renewable energy system for an optimal generation with minimum cost. For the optimal operation of PV systems, the PV array has been set according to the inverter parameters so there is no overvoltage or undervoltage in the system [17–19]. For the inverter oversizing and under-sizing, its rating should be equivalent to installed capacity. For industrial purposes, the solar micro-grid can be beneficial for the prosumer by synchronizing the PV system with the local generator, so the domestic load of micro-grid (maybe an industrial plant) is utilized by synchronized PV system [20]. In fuel cells, hydrocarbons are used to extract hydrogen to be used as fuel while polymer electrolyte membrane has higher energy to be transported to the customer. Other types of fuel cells include direct methanol fuel cells, solid oxide fuel cells, and carbonate type which vary in cost and energy density and for their dynamic operation, a boost converter is used. Fuel cell integration with solar has shown high economic benefits, an energy conversion efficiency of 60–80 percent, scalability to desired demand, and flexibility [21]. So, expeditious deployment of sustainable energy sources sector aided with more mature power electronics in energy sector surely help in meeting energy demands and achieving green environment.

2. Comparison with the Previous Research

In [21], the author proposed a model where PEMFC stack along with solar cell and battery has been incorporated with DC bus to control fluctuations having the drawback of utilization for small scale microgrid. In [22] authors proposed a model for standalone applications where PEMFC is switched by electrolyzer coming from main DC bus where PV Source, PEMFC, and ultracapacitor were feeding to main DC Bus. Authors [23] proposed that integration of PEMFC with solar has shown high economic benefits, energy conversion efficiency of 60–80 percent, scalable to desired demand, and flexible. For the standalone hybrid solar and fuel hybrid system proposed by [24], both sources are synchronized, controlled, and optimized, attached between DC and AC line through an inverter. In our proposed model, PEMFC is synchronized with universal grid and solar energy source for both DC and AC load with energy resource management (ERM) of all sources, making the system effective and reliable for consumer-based load and ECVs utilization. Interference of Grid and introduction to ECVs with renewable sources to overcome any parametric effect of load with the sustainable environment is the motivation for our system.

This research effort discusses the modeling and implementation of grid-connected sustainable energy resources having specific load demand for smart grid utilization. The proposed ERM is discussed in the later sections. A grid connected PEMFC stack is used to increase the ramp rate of the conventional source so line loading can be overcome and the lifetime of that feeder line will be increased. Ramp rate sources are mandatory for industrial zones lines as for domestic purposes there is a negligible ramp rate. At the distribution end, grid-connected non-conventional power sources are placed according to weather conditions with batteries. Non-conventional sources are simulated to check the subsystem efficiency so after integration, losses will be minimal. ECVs battery charging station is integrated with the non-conventional source for stepping towards the sustainable environment as it has a huge attribute in carbon emissions. Line parameters have also been simulated that help in planning and controllability of the system parameters. Modeling of microgrids is done as per location with EVs charging application interfaced with the conventional system to regulate the parameters according to the load demand. It will increase the system reliability by analyzing the efficiency of the non-conventional sources at the simulation tools. Electric charging stations aid in managing the duck curve which arises from conventional resources and to utilize the non-conventional energy resources for which capacity payments are made to the power plant.

3. Proposed Energy Resource Management System

The proposed model is on an AC bus that has multiple sources to overcome the transients and regulated output. The system model constitutes of DERs i.e., PV system and PEM, interfaced with the AC feeder line by DC to AC inverters having maximum power point tracking (MPPT) for specified output voltage. Figure 2 depicts the line diagram of the proposed system. The PV system has multiple series-to-parallel modules while the fuel cell has multiple stacks as per generation capacity. PEMFC has a backup battery as its operations are continuous and can save energy during off-peak hours. The inverter voltage parameter is set according to AC line voltage so these sustainable sources can be synchronized with the grid. The inverter is designed by the IGBT for the application of buck converter, controlled to have constant value at the output. The hydroelectric energy source is also continually feeding to the line by the transformer. PEMFC which has boosted output has fed to the AC line by inverter. The fuel cell is fueled by the hydrogen having electrolyte for production of hydrogen at anode end, so after the reaction water is collected as waste at the cathode.

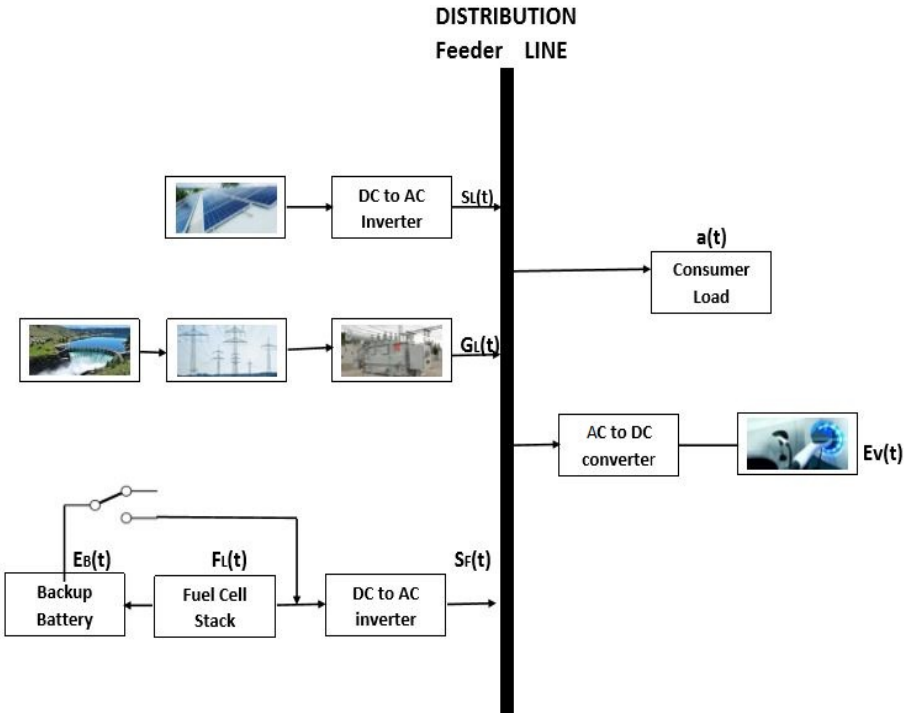

Figure 2. Sustainable distributed energy model for smart grid application.

The AC feeder line voltage is set as a distribution level voltage of 220 V with a line-to-line voltage of 440 V. Transmission line parameters are taken to minimal value for the optimal operation of DERs. The consumer end is modeled by an RLC circuit having power consumption in kW with specified line inductance and capacitance. For a sustainable environment, the electrical vehicle charging module is also interfaced with the AC line through AC to DC converters. The overall system is regularized to meet the AC line load from the sustainable energy resources and using the application of ECVs to have a sustainable environment.

Figure 3 shows the algorithm of the proposed ERM system where conditions have been idealized as system demand for each case of ERM. The priority is given to the PEMFC for high current so the probability of ERM for PEMFC is in a higher range to overcome current ramp conditions of the system. For system stability, priority is given to the grid source to overcome the harmonics and fluctuations in the output. The solar source dependence priority will be given in the caseload to be greater than the grid so in the overall condition of ERM, $Ev(t) + a(t) > SL(t) + GL(t)$, the solar source is incorporated with the grid source as

solar is more economical energy source than others. Solar energy resource has its maximum consumption during daytime when SL(t) = SLmax. The minimum source priority is given to the backup battery as it will be used under its state of charge (SOC) condition. The electrical vehicle module will be a constant load for the system with the variable load of the consumer.

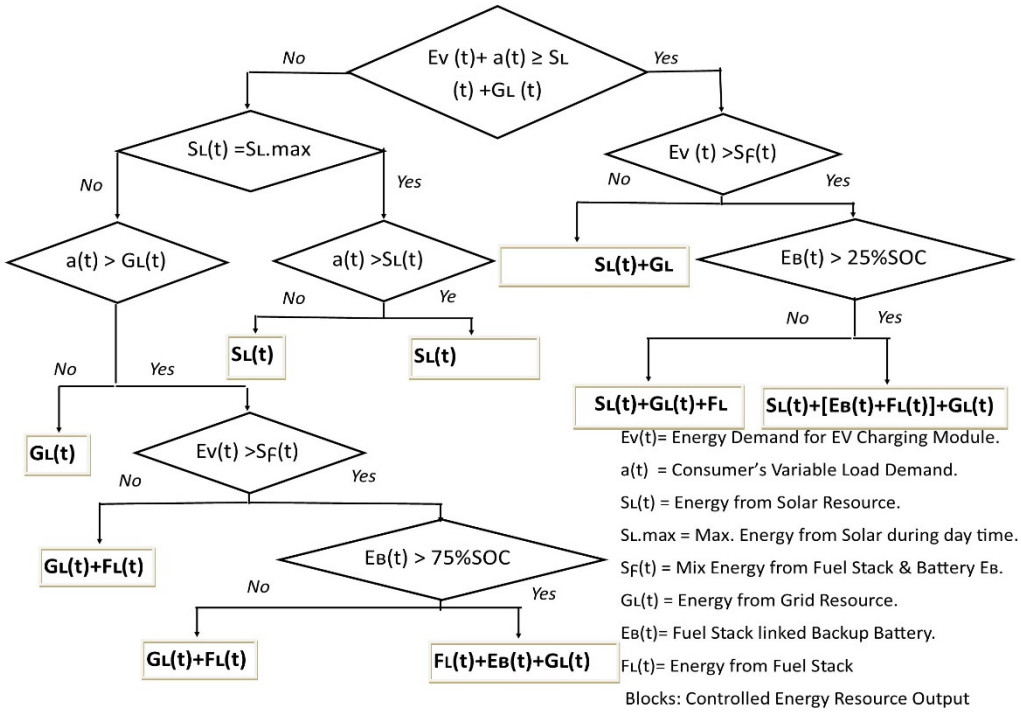

Figure 3. Energy Resource Management Algorithm.

4. Erm System Configuration Parameters and the Simulation Model

The detailed system configuration parameters to model a proposed ERM system are enlisted in Table 1. SN350M-10 solar module with power rating 350 W_p is used in micro-grid modeling, hybrid converters and inverters are being modeled with theoretical power conversion efficiencies of 96% and 85% respectively. PEMFC stack of 6 kW with an efficiency of 60% has been modeled and used for the ERM system. In the proposed system shown in Figure 3, solar resource dependence has a probability of 0.55, fuel cell stack resource has the probability of 0.66, fuel backup battery with the probability of 0.22, the grid is with the probability of 0.88, for the operation of distribution line with varying load demand of consumer and ECVs. The probability of respective energy resources originates from ERM by evaluating the dependence of energy resource for a specific load.

Table 1. Sustainable Sources Specifications.

System	Description
Solar System	Type: SN350M-10, Nominal Power 350 W, Mono Crystalline, Efficiency: 16%, Operating Temp: 50 degree
Fuel Stack	Type: PEM fuel Cell, Power: 6 kW with 45 Vdc output, Fuel: Hydrogen, Efficiency: 60%
Inverter	Three-phase AC Inverter, MPPT Controlled, Life Cycle: 25 years, Efficiency: 85%
AC to DC Converter	Type: 6 pulse Bridge Thyristor, Efficiency: 96%
DC to DC Converter	Type: IGBT controlled Boost converter, Output Voltage: 100 Vdc, Efficiency: 97%

The proposed ERM system shown by the line diagram in Section 3 is implemented and simulated in MATLAB/SIMULINK environment as shown in Figure 4. It can be observed

that PEMFC with battery energy storage system (BESS) or battery stack, ECVs system, and micro-grid is integrated into the local grid. Resource Side Management (RSM) is named for the measurement and results in the analysis section of the ERM system. Further aspects relating to the mathematical modeling of the system are discussed in Section 5.

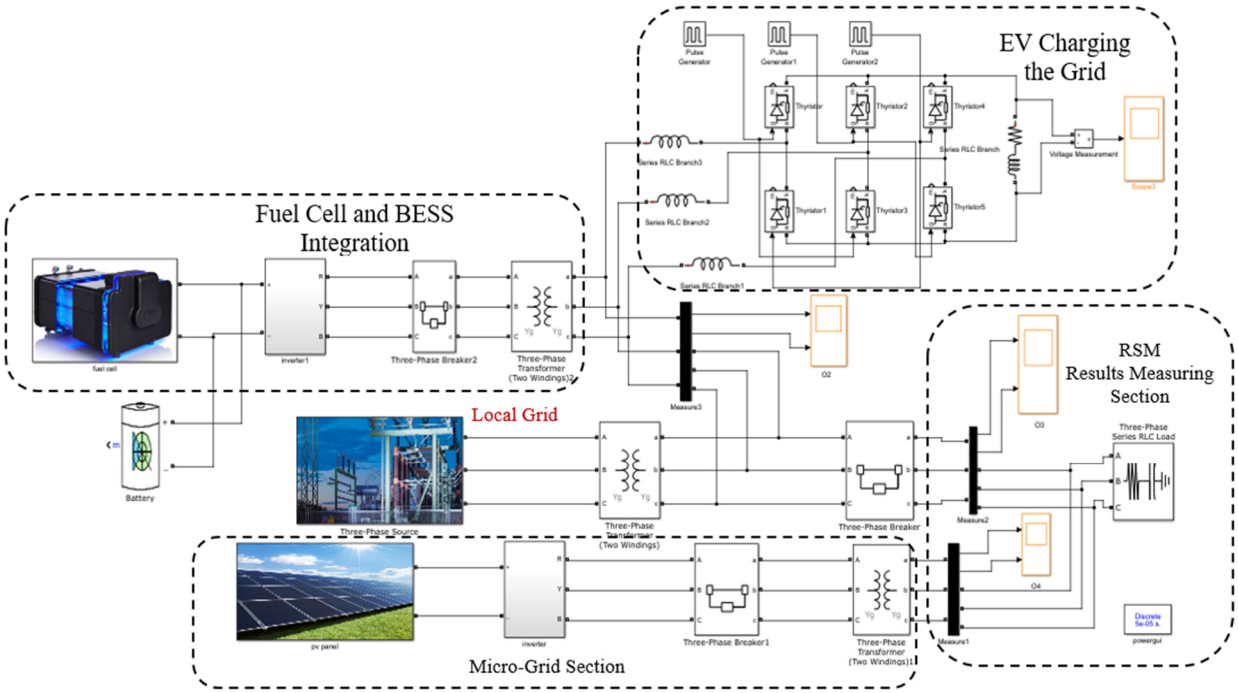

Figure 4. Proposed energy resource management system simulation diagram.

5. Mathematical Modeling and Implementation of Proposed Erm System

PEMFC uses hydrogen as fuel, decomposes hydrogen into protons and electrons at the catalytic layer adjacent to the anode. The oxidant oxygen is accumulated at the cathode catalytic layer, reacts with the hydrogen protons to form water with residual heat too. PEMFC model has a stack of fuel cells with the losses including electrode losses, electrolyte losses, and concentration losses and the circuit model is shown in Figure 5.

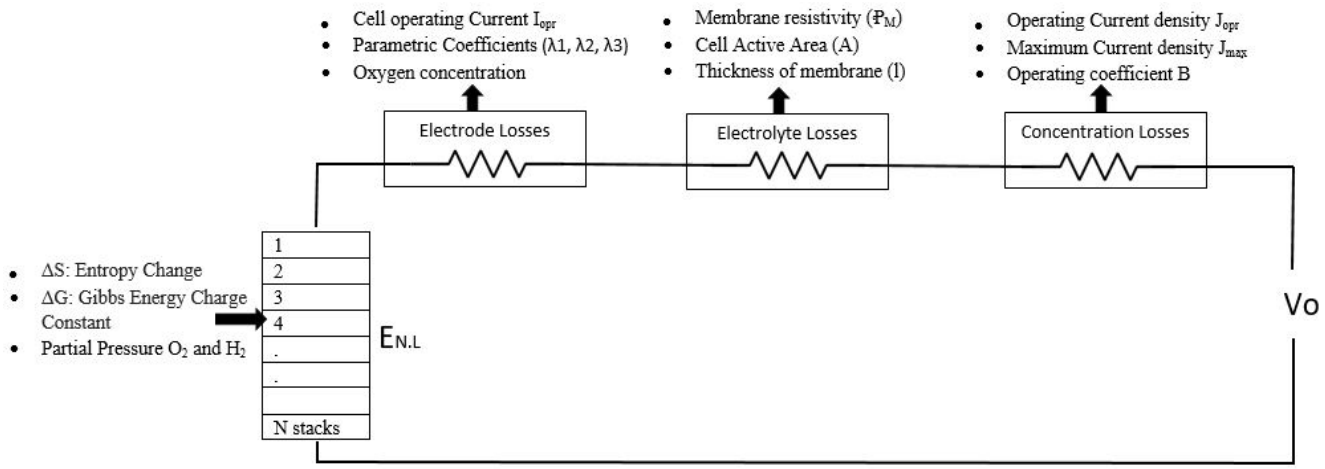

Figure 5. Circuit model of fuel cell stack.

The no-load potential is the open-circuit thermodynamic balance for the standard operating conditions calculated by Nernst Equation. It depends on hydrogen and oxygen

partial pressure and a higher current causes pressure declination with higher temperature. The no-load potential is the reversible voltage of the cell due to Gibbs energy, G, and fuel pressure (i.e., 1.23 V) but due to irreversibility and entropy losses, taken nominal output ranges from 0.9 V to 1.23 V [25]. So, the no-load potential for the operating condition is

$$E_{N,L} = E_{nom} + \frac{\Delta S}{2F}(T - T_0) + \frac{RT}{2F}[ln(P_{H_2}) + \frac{1}{2}ln(P_{o_2})] \quad (1)$$

where

ΔS = Change in entropy (J/mol)
$E_{N.L}$ = Operating open-circuit voltage of fuel cell
E_{nom} = Ideal open-circuit voltage of fuel cell
P_{H_2} = Partial pressure of hydrogen (atm)
P_{O_2} = Partial pressure of oxygen (atm)
R = Universal constant of gases (8.314 J/K mol)
T = Operating temperature of Cell (K)
T_O = Reference temperature of System (K)

As for ideal E_{nom} = 1.23 V so we get,

$$E_{N.L} = 1.23 + 0.0008(T - 298) + 4.3 \times 10^{-5} ln\left[ln(P_{H_2}) + \frac{1}{2}ln(P_{O_2})\right] \quad (2)$$

Equation (1) shows the operating voltage of fuel cells under no-load conditions or reversible conditions. Electrode losses are mainly activation losses as electrode causes the reaction to be slow by diffusion of oxygen at the electrodes and flow channels. Oxygen concentration at catalytic after consideration of diffusion at the electrode is given by Equation (3). Tafel equation has utilized for activation losses result as proposed by [26] in Equation (4).

$$CO_2 = \frac{PO_2}{(5.08)(10^6)\left(e^{\frac{-498}{T}}\right)} \quad (3)$$

$$V_{act} = \begin{array}{c} -0.9514 + 0.00312T - 0.00018Tln(I) \\ +7.4 \times 10^{-5} Tln(CO_2) \end{array} \quad (4)$$

Electrolytic losses mainly refer to the resistance of protons through the membrane and electrons through the external circuit of fuel cell constitute ohmic losses. The empirical equations proposed by [27] were used to find membrane-specific resistance and parametric constants for membrane Area.

$$V_{ohmic} = I(Rm + Rc) \quad (5)$$

where

A = Active area of the cell (cm^2)
l = Thickness of fuel cell membrane (cm)
R_m = Resistance of the membrane (Ω)
R_c = Resistance of electrode connections (Ω)
V_{act} = Activation voltage drop in fuel
V_{ohmic} = Ohmic losses through the PEMFC

There is a maximum limit of fuel consumption for which maximum current density is allocated. For the maximum current, huge mass transport of fuel causes the drop of the partial pressure of H2 and O2 at electrodes.

$$V_{con} = -Bln\left(1 - \frac{J}{J_{max}}\right) \quad (6)$$

where

B = Parametric constant for cell operation
J = Actual current density of cell (A/cm^2)
J_{max} = Maximum current density of cell (A/cm^2)
V_{con} = Concentration losses

So, the output operational voltage of the fuel cell stack shown in the circuit model in Figure 5 is formalized in Equation (7) with single cells, connected layer by layer. Simulink modeling of PEMFC for the above-formularized model is shown in Figure 6.

$$V_{out} = N(E_{NL} - V_{act} - V_{ohmic} - V_{con}) \tag{7}$$

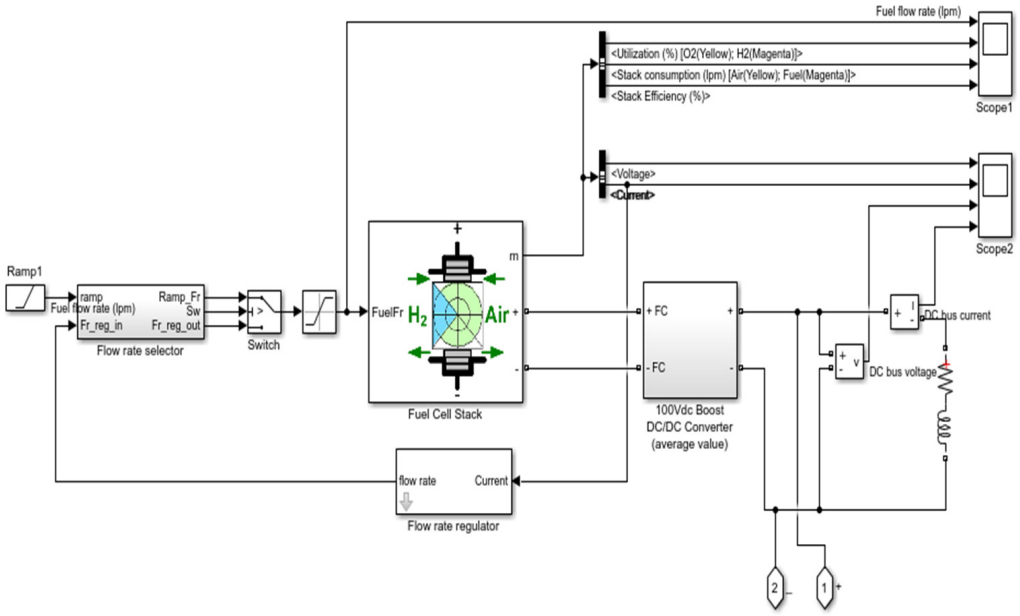

Figure 6. Simulink model of fuel stack.

Multiple connections of solar cells constitute solar panels while the placement of solar panels in parallel-series connections constitutes a solar system. As with fuel cells, a single-cell model is considered for solar system modeling with series and shunt resistance for internal resistance and leakage losses, respectively.

$$I = I_{ph} - [I_s \times exp^{\frac{(q(V+R_sI))}{aV_{th}}} - 1] - \frac{V + R_s\, I}{R_{sh}} \tag{8}$$

where

I = Current across single solar cell/current across the single fuel cell
I_{ph} = Current produced by shinning photons
R_{sh} = Shunt resistance of a solar cell
R_s = Series resistance of a solar cell
V = Voltage across the single solar cell
V_{th} = Thermal voltage
q = Charge of an electron

The output current will be a difference of shunt current and diode current from the PV source current.

$$I = N_pI_{ph} - [N_pI_s \times exp^{\frac{(q(V+R_sI))}{aV_{th}}} - 1] - \frac{V + R_s\, I}{R_{sh}} \tag{9}$$

where

I_s = Solar cell reverse saturation current
N_p = Parallel connected solar panels

For the Grid connection of RERs, boost converters are used for the application to control specific parameters at the output. For the PV voltage or fuel voltage V_{rer} and inductor current I, boost converter can be modeled mathematically as [28].

$$\frac{dV_{rer}}{dt} = \frac{1}{C_{rer}}(I_L - I_{rer}) \tag{10}$$

$$\frac{dI}{dt} = \frac{1}{L_{rer}}(V_{mpp} - V_{rer}) - \frac{R_{rer}}{L_{rer}})I_L \tag{11}$$

where

C_{RER} = Renewable source shunt capacitance
I_L = Inductor current of a boost converter
L_{RER} = Series inductance of renewable resources
V_{RER} = Voltage from fuel stack or solar array

For the optimization of DERs, the single cell-based optimization is modeled for the PEMFC and PV systems. As MPPT tracking is to optimize the power output in PV, the ideal MPPT point is achieved for specific Vmpp by considering the optimal value of Rs and Rsh to get optimal Ipv by Equation (9) [29]. The relation between Rs and Rsh for the optimal MPPT point is given as Equation (12).

$$R_{sh} = \frac{V_{mpp}\left(V_{mpp} - I_{mpp} \cdot R_s\right)\frac{N_s}{N_p}}{\frac{N_s}{N_p}\left[V_{mpp}(I_{sc} - I_d)\right] - P_{mpp}} \tag{12}$$

where

I_d = Saturation current of diodes in the array
I_{mpp} = Maximum power point of the current
N_s = Series connected solar panels
V_{mpp} = Maximum power point of voltage
I_{sc} = Short circuit current of a panel in the array
P_{mpp} = Maximum power point of solar cell

The demand current, I_{demand} of fuel cell stack varies with the constant factors and hydrogen utilization which is given as.

$$I_{demand} = \frac{U_{opt}}{2B}(q_{h_2}) \tag{13}$$

where

B = Parametric constant for cell operation
q_{h_2} = Fuel Flow Rate
U_{opt} = Optimal utilization of PEMFC energy

The optimal range of demanded current in the PEMFC depends on the partial pressure of hydrogen and optimal utilization of hydrogen. The minimum and maximum optimal range of hydrogen cell utilization is 80% to 90% taking operational constraints for overused fueling, underused fueling, and under voltages.

$$\frac{(0.8q_{h_2})}{2B} = I_{min} \leq I_{demand} \leq I_{max} = \frac{(0.9q_{h_2})}{2B} \tag{14}$$

The operating power delivered to the grid by fuel stack is formulated by output stack voltage shown in Equation (7) and fuel current dependent on input fuel rate. The solar power is extracted after power conditioning losses and array losses including inverter

operating efficiency at the AC bus. So the power at the distribution end of DERs shown in Figure 4 incorporating the power losses is mathematically modeled as;

$$P_{grid} = [P_{pv}(1 - \lambda_p)(1 - \lambda_c) + I_{FC}(V_{out})\eta_{in}] \quad (15)$$

where

η_{inv} = Inverter Efficiency
λ_c = Power Conditioning Losses
λ_p = Photovoltaic Array Losses
I_{FC} = Fuel Generated Current
P_{grid} = Power Delivered to Grid
P_{pv} = Extracted Solar Power

The thyristor-based rectifier model is implemented for EVs fast-charging whose DC link voltage is dependent on the cosine of firing angle which has six ripple pulses per frequency cycle and is shown in Figure 7.

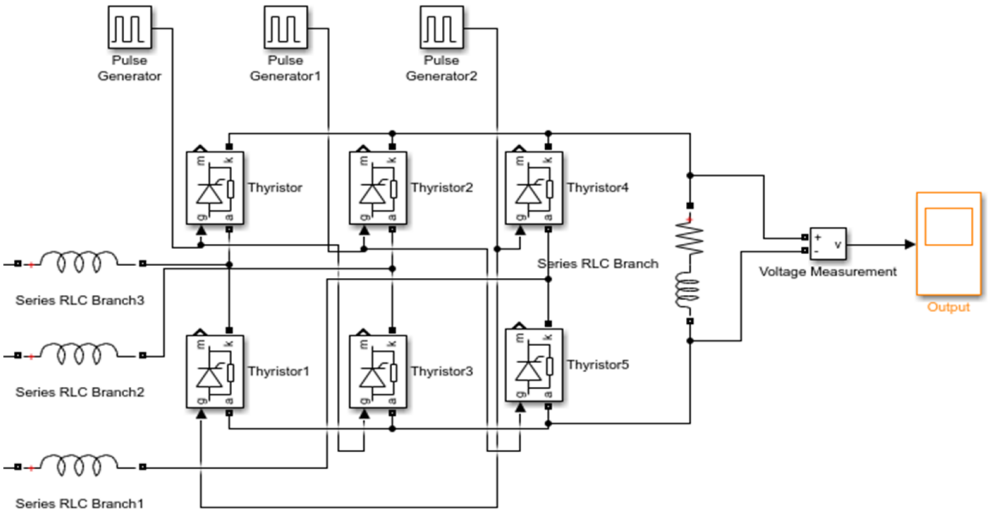

Figure 7. Thyristor based model of electrical vehicle charging.

6. Simulation Results and Discussions

PEMFC with its backup source will be utilized during Ev(t) > SF(t) as shown in Figure 3, in case SL(t) + GL(t) is not meeting the ramp load of charging modules during Ev(t) + a(t) > SL(t) + GL(t) condition. While in case of Ev(t) + a(t) < SL(t) + GL(t), load demand of Ev(t) and a(t) can be fulfilled without the backup sources. As EVs modules rating depends on Ampere-hour which can be achieved by the current ramp of fuel cell stack with its backup. For the simulation of PEMFC, the stack of 65 cells coupled for 45 V DC nominal voltage with 55% stack efficiency, is linked with a boost converter for higher average DC voltage. PEMFC is regulated by a flow rate selector having ramp input and flow rate regulator for the current. Figure 5 output of boost voltage interfaced with fuel Stack designed by chopper circuit, controlled by the duty cycle. As the DC bus voltage becomes steady after few transients to give a regulated output which gives a pure sinusoidal wave with no distortion. The chopper circuit makes the lossless DC to DC conversion which is best suitable for the above cases. The DC bus voltage is shown in Figure 8.

The DC bus current for the above condition EV(t) > SF(t) is shown in Figure 9 which is simulated for PEMFC with its backup source utilization for load consumption. EVs modules are ampere-hour dependent which can be fulfilled by the ramp rate of the fuel cell stack. The output wave has zero harmonic distortion for the regulated output. Only

switching losses can be incorporated for ramp current output and steady DC output of PEMFC which has minimal value.

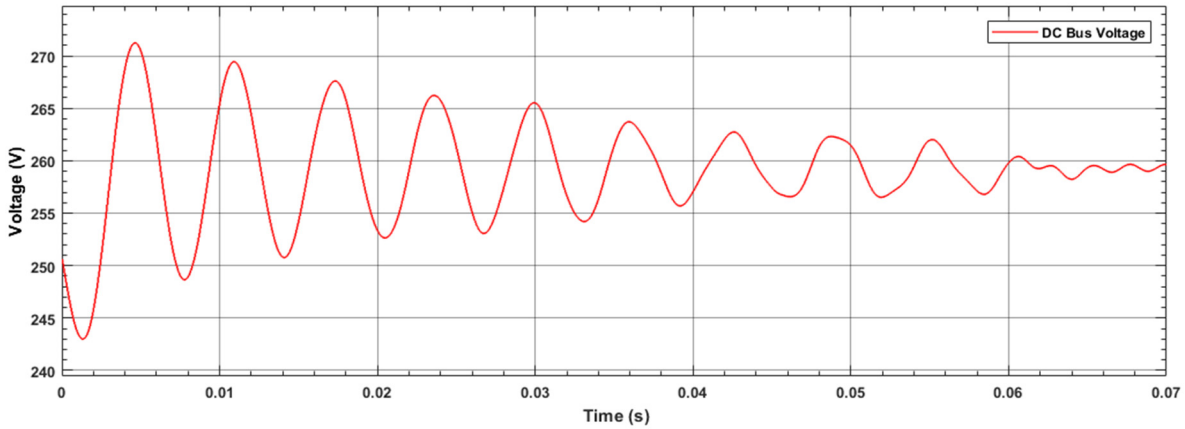

Figure 8. Boosted fuel cell output of DC bus.

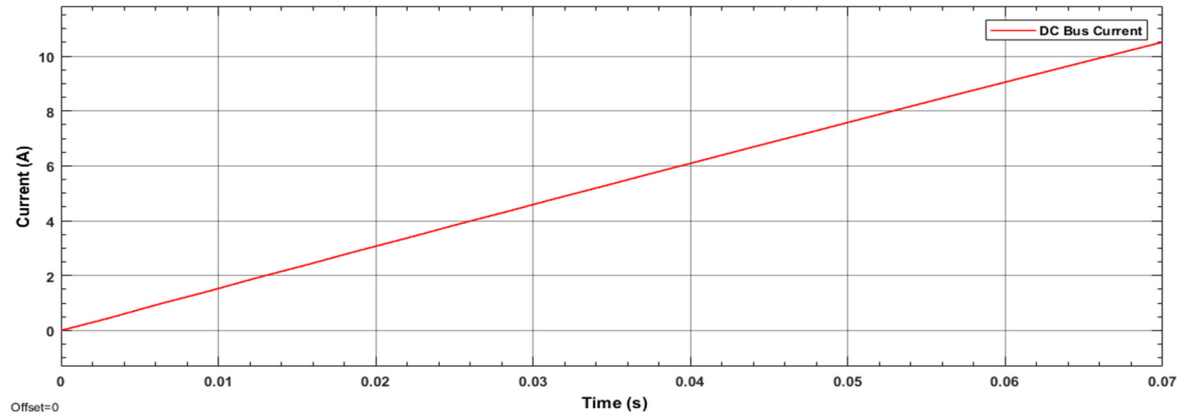

Figure 9. Boosted PEMFC output of DC bus.

Inverters are connected with each solar energy resource and PEMFC for the power conditioning as shown in Figure 2. Both inverters convert the DC power of resources to AC power for the distribution feeder line. The inverted output as per load demand is shown in Figure 10. Both inverters will be operated under Ev(t) + a(t) > GL(t) + SL(t) condition while for other conditions, it depends on resource management. As solar resource connected inverter operation mainly depends on load requirement a(t) and PEMFC connected inverter operated as per ampere-hour-based load of EV modules. Whereas in between grid has continuous energy resource. Cases for different operating conditions which are shown in the ERM algorithm are discussed and simulated below. 5

A three-phase IGBT-based inverter is modeled for the conversion of DERs to AC power, modeled in MATLAB with LC filter at the output to minimize the ripple and smoothing of output. LC filter is coupled with closed-loop proportional integral derivative (PID) Controller and pulse width modulation (PWM) generator, given at gate terminal of IGBT. Both fuel cell stack and solar panels are integrated with an inverter of the same conditions for the synchronized output whose DC voltage, inverter output, filtered output, and modulation index is shown in Figure 10. IGBT inverter has only conduction and switching losses which has minimal value with no effect on inverter output. The IGBT switching gives the maximum value of the voltage to the load bus for peak load conditions so the system meets the demand of load effectively.

Three-phase breakers are interfaced at the DERs line for the optimal control of the system while not interfaced at the gridline of the hydroelectric source as a basic methodology is to synchronize the sources into the grid. Peak and off-peak hours can be adjusted for the optimal control of DERs. All loads cannot be shifted to DER as highly inductive load make the DER system unstable. The transformer connected with the AC bus has a Y-Y winding connection with minimal parameters and has a rating greater than the load components. EV charging module has assumed the same parameters as for the battery including initial state, terminal state, maximum charging, and minimal charging for the optimal control of the system.

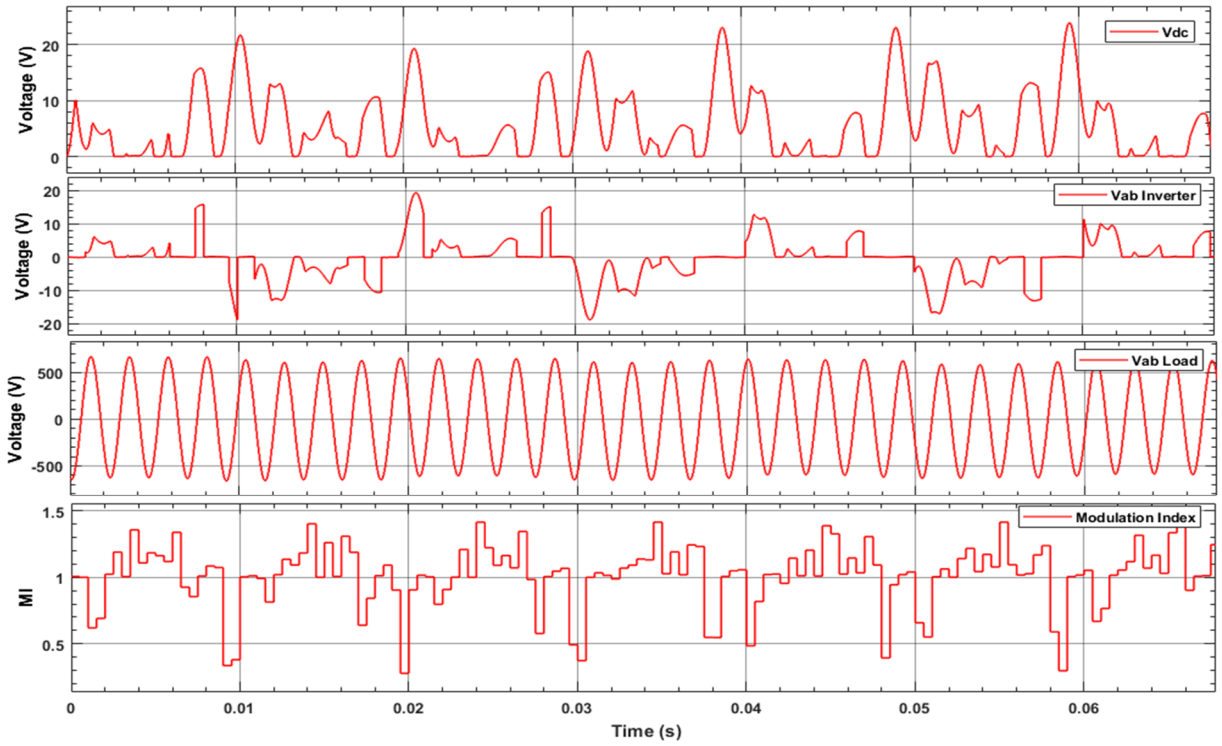

Figure 10. Inverter conditioning graphs.

EV charging module for smart grid utilization is taken as DC load for the grid whose output from thyristor model as simulated in SIMULINK is shown in Figure 11. EVs charging energy is taken as ampere hour-based load whose concentration is mainly fulfilled by fuel stack and its backup battery having a high ramp rate. For the operation of the grid having load demand less than PEMFC resource, demand to be fulfilled by solar and grid but for EVs demand equal or greater than PEMFC, demand is fulfilled by all resources with the backup battery too. The constant current demand of the electrical vehicle module is met by the source with regulated DC output at the output terminal. For the DC output, the thyristor-based model is utilized whose output is shown in Figure 11.

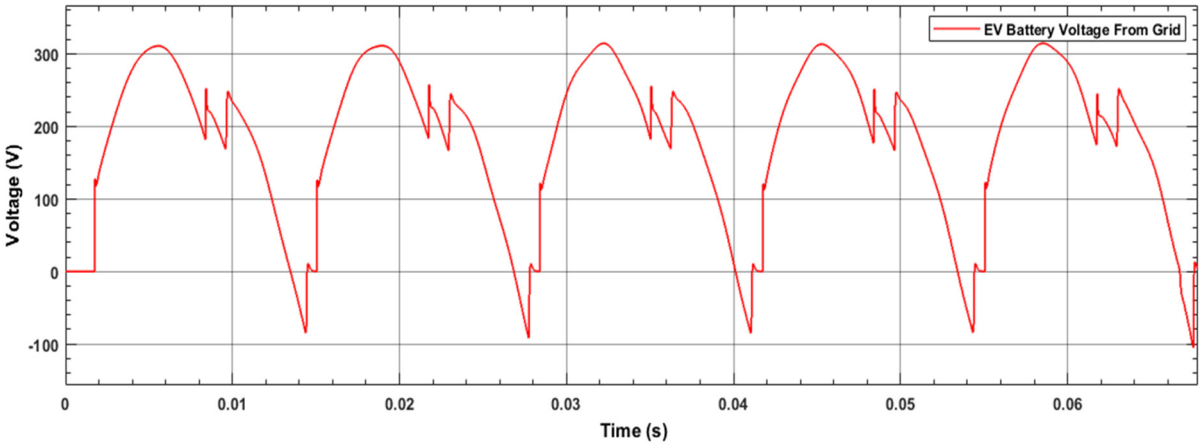

Figure 11. Electrical vehicle battery voltage from grid.

The smart ERM flow chart depicted in Figure 3 illustrates the conditions to control DERs with respective power demands. Solar can be utilized when it is operating with a maximum output which is consumed when a load is less than the solar resource. Solar interference is mandatory in case of a load being less than solar otherwise load will have to shift to grid resource. For the load to be greater than both solar and grid, a choice of fuel Stack resource is also added with the backup battery. It has been inferred that under different operating conditions has voltage regulation less than 5% with minimal ripple waveform. Power conditioning equipment's simulations show its optimal working efficiency with less than 1% losses as shown by fuel cell stack simulations and inverter output. A backup battery is given preference in case of a load to be greater than solar and grid by discharging until 25% of the state of charge (SOC), as in other caseload is already less than solar and grid resource so here battery can discharge until 75% of SOC. For the load to have all resources attached to the grid for the load, the voltage and current output graphs are shown as calculated for the load in equation 16.

For the operating condition of consumer load and ECV with fuel cell stack, the situation is taken for the EVs and consumer load both to be greater than Solar and Grid EV(t) + a(t) > SL(t) + GL(t). All the DERs SL(t) + GL(t) + [FL(t) + EB(t)] are stacked for the balanced output. The DERs are integrated with the distribution AC bus, connected with the load end and ECVs module. Six pulses thyristor-based model is used for EVs and load is denoted by the RLC circuit. The Load is considered to a distribution end load of 200 KW with the fixed bus line to line voltage of 440 KV. So, the current demand of load is formulated as

$$I_{Load} = 200\ \text{KW} / V_{Load} = 200\ \text{KW} / 440\ \text{V} = 454\ \text{A} \quad (16)$$

As shown by Figure 12 for meeting the demand of load with PEMFC, grid, and solar dependence, the waveform is pure sinusoidal and accurate for a load of Equation (16)For the operating condition of consumer load and electrical vehicle charging module without fuel cell stack, the output waveform is shown in Figure 13.

The output current has decreased to a significant value as the ramp source of current of PEMFC has been cut off from the system. In other conditions, the current source of the load can be met as to cut off the solar source show less regulation in the output wave. As the consumer is power factor controlled and EVs load has a current dependency, so the PEMFC source can be mandatory for the stable and balanced output waveform. The fuel cell stack source has a dependence of 66% which must be mantled in a system under maximum cases except for S(t) = SLmax under the condition of Ev(t) + a(t) < SL(t) + GL(t). For the operating condition of consumer load and EV charging module without grid source, the output waveform is shown in Figure 14.

Under this operating condition, the output waveform is not pure sinusoidal as the waveform shows harmonic losses. This condition is least interested as shown in ERM

in Figure 3 that Grid source dependence should have a dependence of 0.88 for efficient power flow without any losses. For the operating condition without PEMFC, the current demand is not meeting so has less value of current at the output. while the operating condition without a grid source has harmonic losses and nonregulated output. So from these outputs, the ERM dependence of each source can be easily evaluated and cross verified with Figure 3. While the backup source utilization depends on its SOC so has minimal dependence of all with a 0.22 working probability.

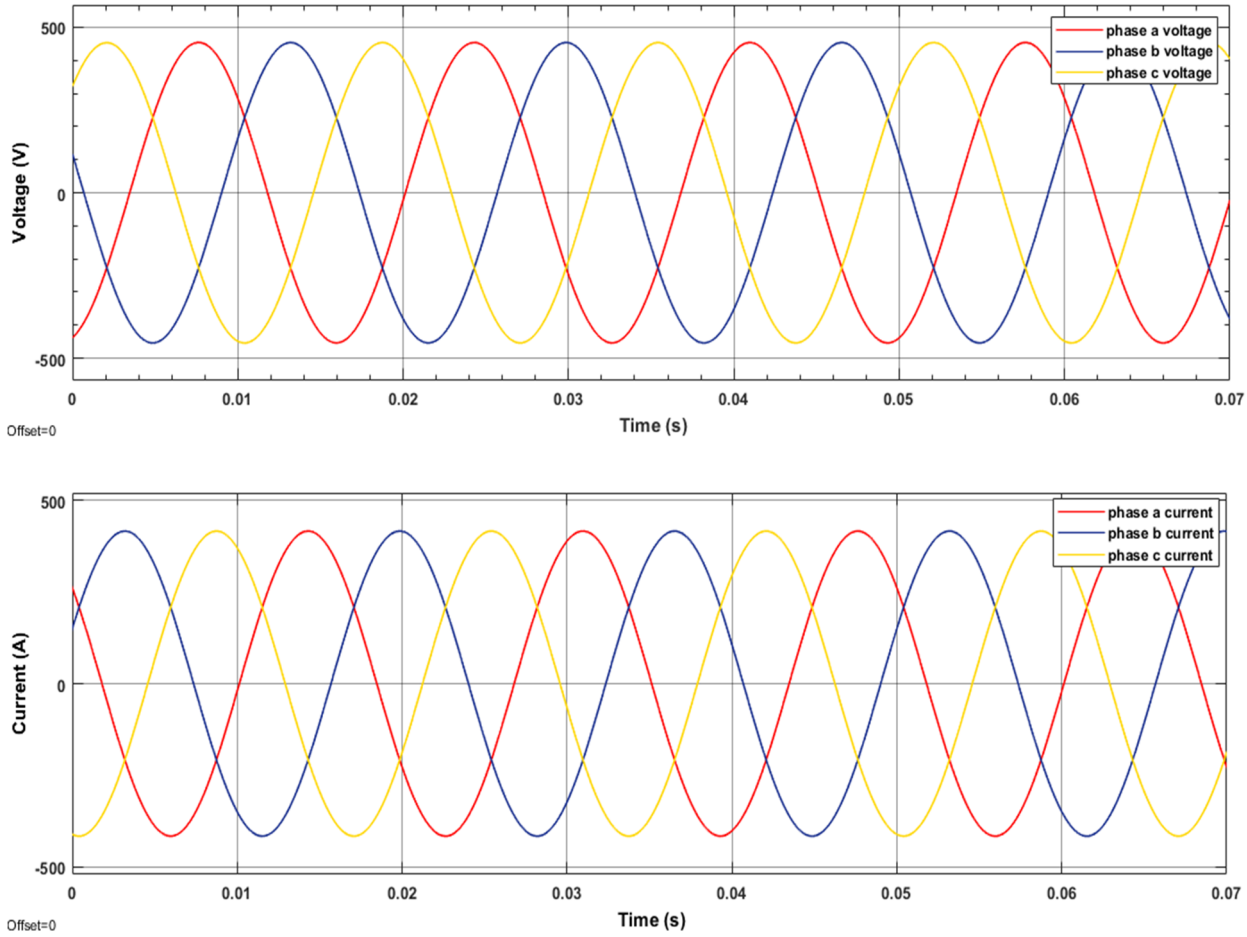

Figure 12. Phase to phase voltage and current as calculated in Equation (16).

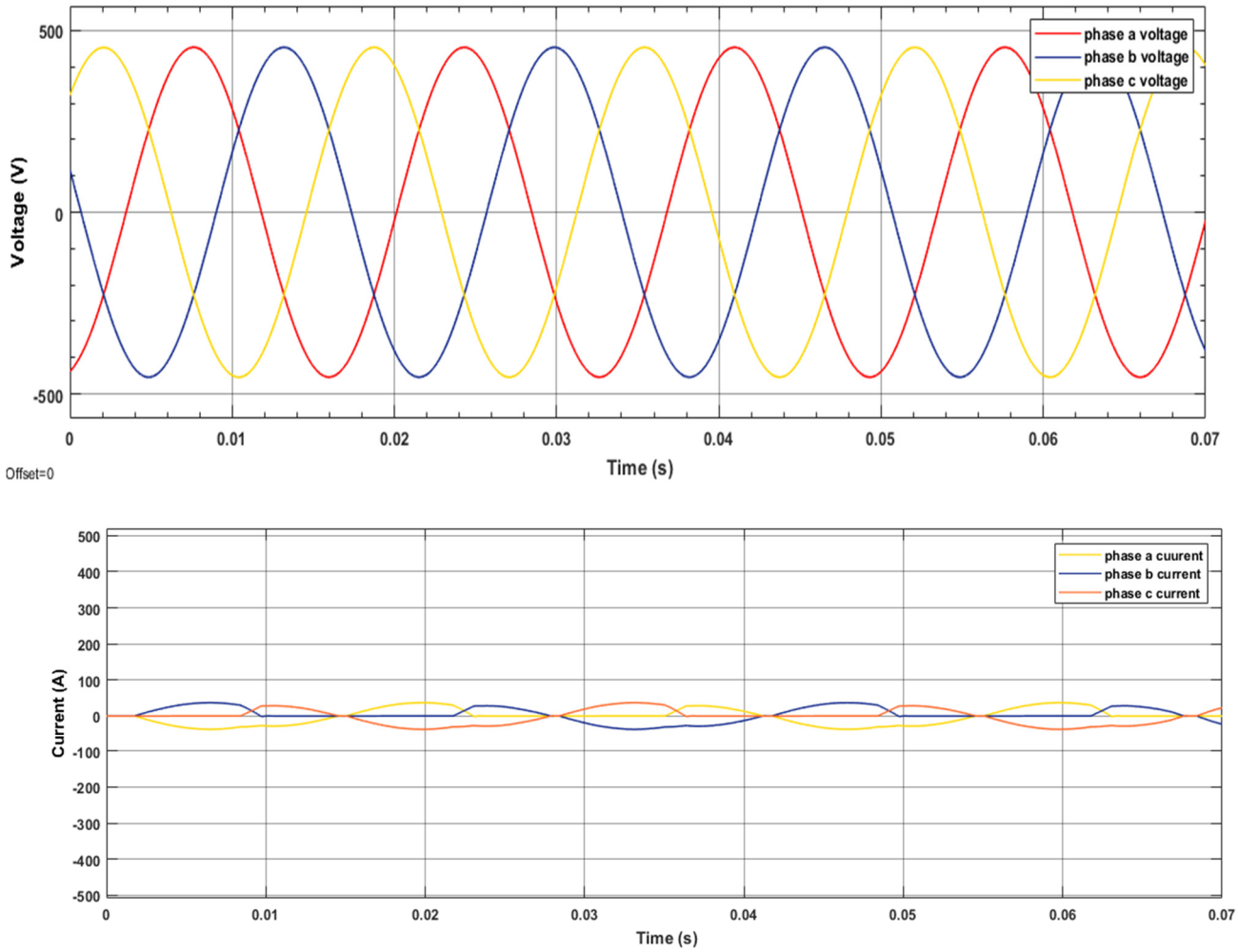

Figure 13. Phase to phase voltage and current for condition without PEMFC.

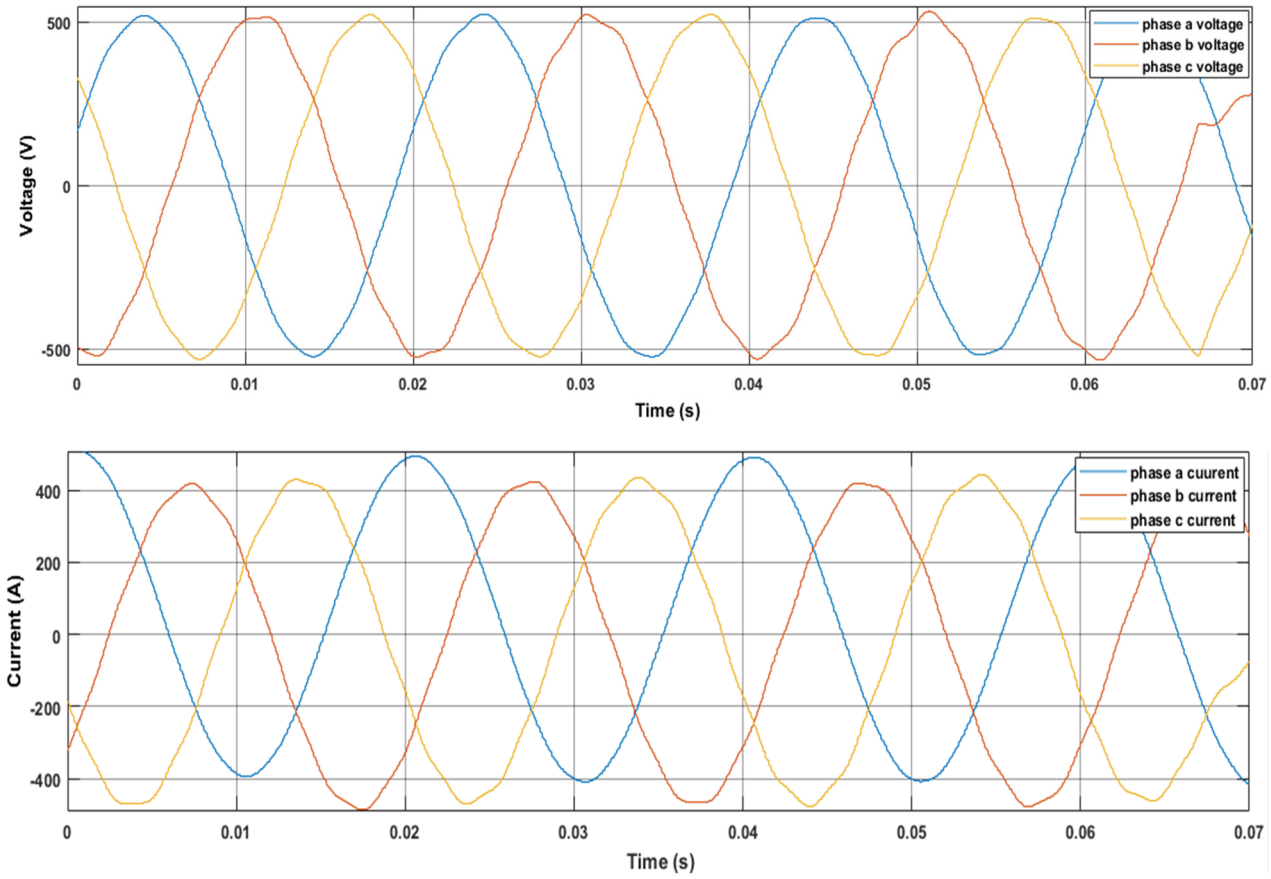

Figure 14. Phase to phase voltage and current for condition without grid source interference.

7. Conclusions

An alternative distributive energy model is proposed which is better than the usual distribution system for making the system reliable, flexible, and economical with less transmission line cost and losses. Simulation of the model under operating conditions of DERs concerning utilization i.e., DERs with PEMFC, DERs without PEMFC, DERs without grid source, has a pure sinusoidal waveform with minimal ripple factor, minimal harmonic distortion, and regulated output as per load demand. Besides the efficiency of DERs as specified in Table 1, there is minimal harmonic distortion (<1%) as seen from its waveforms and minimal line losses in the system consisted of IGBT-based inverter and converters used for pure sinusoidal and regulated output. Simulation of DERs is done for the specific load in SIMULINK, with resources to be modeled with optimal parameters. The probability of sources for efficient ERM has been confirmed by simulating the proposed model under different operating conditions, by which the grid dependence is prior of all with 0.88 probability to nullify harmonic losses, fuel source dependence of 0.66 for meeting the high current ramp rate as per a load of ECVs and consumer while the solar source has 0.55 dependence as solar has less capacity of all sources. This model can be adapted in countries whose past energy dependence on the national grid, to increase System reliability and become Energy unit more economical by ERM. Distributed system resources interfaced with ECVs by ERM leads to cost-effectiveness and sustainability. This model is implementable in any weak micro-grid for a regulated output with low power loss as implemented in the paper. The scope of the proposed model can be extended by analyzing the proposed model to find the Power flow. This will decrease energy cost, minimize losses and maximize reliability for weak micro-grids.

Author Contributions: H.A.T.: data curation, formal analysis, investigation, methodology, project administration, resources, software, validation, visualization, writing—original draft, writing—review and editing, F.S.: conceptualization, data curation, formal analysis, investigation, methodology, project administration, resources, software, validation, visualization, writing—original draft, writing—review and editing M.H.Y.: conceptualization, investigation, formal analysis, software, visualization, writing—original draft, writing—review and editing. A.I.: conceptualization, investigation, formal analysis, software, visualization, writing—original draft, writing—review and editing H.A.: conceptualization, investigation, formal analysis, software, visualization, writing—original draft, writing—review and editing M.H.K.: investigation, formal analysis, visualization, writing—original draft, writing—review and editing H.E.G.: conceptualization, methodology, formal analysis, investigation, writing—review and editing, supervision. All authors have read and agreed to the published version of the manuscript.

Funding: This research did not receive any specific grant from funding agencies in the public, commercial, or not-for-profit sectors.

Conflicts of Interest: The authors declare no conflict of interest.

Nomenclature

A	Active Area of Cell (cm^2)
AQI	Air Quality Index
AC	Alternating Current
a(t)	Consumers variable load demand
BESS	Battery Energy Storage System
DC	Direct Current
DERs	Distribution Energy Resources
FL(t)	Energy from Fuel Stack
G	Gibbs Energy
ΔG	Change in Gibbs Free Energy for useful work (J/mol)
GL(t)	Energy from Grid Source
HVDC	High Voltage Direct Current
η_{inv}	Inverter Efficiency
λ_c	Power Conditioning Losses
λ_p	Photovoltaic Array Losses
ρ_m	Specific Resistance for the Electrons through the Fuel Membrane (Ω-cm)
B	Parametric Constant for Cell Operation
CO_2	Oxygen Concentration at the Cathode Catalytic side (mol/cm^3)
ERM	Energy Resource Management
EB(t)	Fuel Stack Linked Battery
C_{RER}	Renewable Source Shunt Capacitance
Ev(t)	Energy Demand of Charging module
$E_{N.L}$	Operating Open Circuit Voltage of Fuel Cell
ECVs	Electrical Charging Vehicles
EVs	Electric Vehicles
E_{nom}	Ideal Open Circuit voltage of fuel Cell
F	Faraday Constant (96.487)
IGBT	Insulated Gate Bi-polar Thyristor
I	Current across single solar cell/Current across Single Fuel Cell
I_d	Saturation Current of Diodes in Array
I_{FC}	Fuel Generated Current
I_{load}	Consumer Load Current
I_L	Inductor Current of Boost Converter
I_{mpp}	Maximum Power Point of Current
I_{ph}	Current produced by shinning Photons
I_{sc}	Short Circuit Current of Panel in Array
I_s	Cell Reverse Saturation Current
J	Actual Current density of Cell (A/cm^2)

J_{max}	Maximum Current density of Cell (A/cm^2)
l	Thickness of Fuel Cell Membrane (cm)
L_{RER}	Series Inductance of Renewable Resource
MPPT	Maximum Power Point Tracking
N_p	Parallel Connected Solar Panels
N_s	Series Connected Solar Panels
PV	Photovoltaic
PEMFC	Proton Exchange Membrane Fuel Cell
PID	Proportional Derivative Integrator
PWM	Pulse Width Modulation
P_{grid}	Power Delivered to Grid
P_{h_2}	Partial Pressure of Hydrogen (atm)
P_{mpp}	Maximum Power Point of Solar Cell
P_{O_2}	Partial Pressure of Oxygen (atm)
P_{pv}	Extracted Solar Power
q_{h_2}	Fuel Flow Rate
R	Universal Constant of Gases (8.314 J/K mol)
RERs	Renewable Energy Resources
RSM	Resource Side Management
R_c	Resistance of Electrode Connections (Ω)
R_m	Resistance of Membrane (Ω)
R_{RER}	Renewable Source Resistance
R_{sh}	Shunt Resistance of Solar Cell
R_s	Series Resistance of Solar Cell
SOC	State of Charge
ΔS	Change in Entropy (J/mol)
SL(t)	Energy from Solar Resource
SL.max	Maximum Energy from Solar during Day Time
SF(t)	Mix Energy From Fuel Stack and Battery EB
T	Operating Temperature of Cell (K)
T_O	Reference Temperature of System (K)
U_{opt}	Optimal Utilization of Fuel Cell Energy
V	Voltage across Single Solar Cell
V_{act}	Activation Voltage Drop in Fuel
V_{con}	Concentration Losses
V_{th}	Thermal Voltage
V_{mpp}	Maximum Power Point of Voltage
V_{ohmic}	Ohmic Losses through the Fuel Cell
V_{RER}	Voltage from Fuel Stack or Solar Array

References

1. Upadhyay, S.; Sharma, M.J.R.; Reviews, S.E. A review on configurations, control and sizing methodologies of hybrid energy systems. *Renew. Sustain. Energy Rev.* **2014**, *38*, 47–63. [CrossRef]
2. Yousuf, I.; Ghumman, A.; Hashmi, H.; Kamal, M.J.R.; Reviews, S.E. Carbon emissions from power sector in Pakistan and opportunities to mitigate those. *Renew. Sustain. Energy Rev.* **2014**, *34*, 71–77. [CrossRef]
3. Huld, T.; Jäger Waldau, A.; Ossenbrink, H.; Szabo, S.; Dunlop, E.; Taylor, N. Cost maps for unsubsidised photovoltaic electricity. *Eur. Comm.* **2014**.
4. Aziz, A.; Bajwa, I.U. Energy and pollution control opportunities for Lahore. *Wit Trans. Built Environ.* **2004**, 75.
5. Novoa, L.; Flores, R.; Brouwer, J. Optimal renewable generation and battery storage sizing and siting considering local transformer limits. *Appl. Energy* **2019**, *256*, 113926. [CrossRef]
6. Sbordone, D.; Bertini, I.; Di Pietra, B.; Falvo, M.C.; Genovese, A.; Martirano, L. EV fast charging stations and energy storage technologies: A real implementation in the smart micro grid paradigm. *Electr. Power Syst. Res.* **2015**, *120*, 96–108. [CrossRef]
7. Wang, Y.; Huang, Y.; Wang, Y.; Zeng, M.; Li, F.; Wang, Y.; Zhang, Y. Energy management of smart micro-grid with response loads and distributed generation considering demand response. *J. Clean. Prod.* **2018**, *197*, 1069–1083. [CrossRef]
8. Elakya, A.; Srikeerthana, K.; Santhiya, R.; Sanjeevkapoor, S.; Ragul, M. Efficient Power Electronic Converter for Electric Vehicle Applications with Energy Storage Systems. In Proceedings of the 2020 6th International Conference on Advanced Computing and Communication Systems (ICACCS), Coimbatore, India, 6–7 March 2020; pp. 935–939.

9. Ghosh, A.; Erickson, R.W. Drive cycle based reliability analysis of composite dc-dc converters for electric vehicles. In Proceedings of the 2020 IEEE Transportation Electrification Conference & Expo (ITEC), Chicago, IL, USA, 23–26 June 2020; pp. 544–549.
10. Vernica, I.; Wang, H.; Blaabjerg, F. A Mission-Profile-Based Tool for the Reliability Evaluation of Power Semiconductor Devices in Hybrid Electric Vehicles. In Proceedings of the 2020 32nd International Symposium on Power Semiconductor Devices and ICs (ISPSD), Vienna, Austria, 17–21 May 2020; pp. 380–383.
11. Hariri, R.; Sebaaly, F.; Kanaan, H.Y. A Review on Modular Multilevel Converters in Electric Vehicles. In Proceedings of the IECON 2020 The 46th Annual Conference of the IEEE Industrial Electronics Society, Singapore, 18–21 October 2020; p. 4987-1993.
12. Kamel, A.A.; Rezk, H.; Abdelkareem, M.A. Enhancing the operation of fuel cell-photovoltaic-battery-supercapacitor renewable system through a hybrid energy management strategy. *Int. J. Hydrog. Energy* **2020**, *46*, 6061–6075. [CrossRef]
13. Moazeni, F.; Khazaei, J. Electrochemical optimization and small-signal analysis of grid-connected polymer electrolyte membrane (PEM) fuel cells for renewable energy integration. *Renew. Energy* **2020**, *155*, 848–861. [CrossRef]
14. Du, Y.; Lu, X.; Wang, X. Power system operation with power electronic inverter–dominated microgrids. In *New Technologies for Power System Operation and Analysis*; Elsevier: Amsterdam, The Netherlands, 2020; pp. 259–274.
15. Jain, H.; Bhatti, B.A.; Wu, T.; Mather, B.; Broadwater, R.J.E. Integrated Transmission-and-Distribution System Modeling of Power Systems: State-of-the-Art and Future Research Directions. *Energies* **2020**, *14*, 12. [CrossRef]
16. Yadav, M.; Pal, N.; Saini, D.K. Microgrid Control, Storage, and Communication Strategies to Enhance Resiliency for Survival of Critical Load. *IEEE Access* **2020**, *8*, 169047–169069. [CrossRef]
17. Kumar, R.; Rajoria, C.; Sharma, A.; Suhag, S. Design, and simulation of standalone solar PV system using PVsyst Software: A case study. *Mater Today Proc.* **2020**. Available online: https://www.sciencedirect.com/science/article/pii/S2214785320366700 (accessed on 10 April 2021).
18. Sharma, R.; Sharma, S.; Tiwari, S. Design optimization of solar PV water pumping system. *Mater. Today Proc.* **2020**, *21*, 1673–1679. [CrossRef]
19. Siregar, Y.; Hutahuruk, Y. Optimization Design and Simulating Solar PV System Using PVSyst Software. In Proceedings of the 2020 4th International Conference on Electrical, Telecommunication and Computer Engineering (ELTICOM), Medan, Indonesia, 3–4 September 2020; pp. 219–223.
20. Mohamed Hariri, M.H.; Mat Desa, M.K.; Masri, S.; Mohd Zainuri, M.A.A. Grid-Connected PV Generation System—Components and Challenges: A Review. *Energies* **2020**, *13*, 4279. [CrossRef]
21. Ferahtia, S.; Djerioui, A.; Zeghlache, S.; Houari, A. A hybrid power system based on fuel cell, photovoltaic source, and supercapacitor. *SN Appl. Sci.* **2020**, *2*, 1–11. [CrossRef]
22. Akinyele, D.; Olabode, E.; Amole, A. Review of Fuel Cell Technologies and Applications for Sustainable Microgrid Systems. *Inventions* **2020**, *5*, 42. [CrossRef]
23. Li, Z.; Zheng, Z.; Xu, L.; Lu, X. A review of the applications of fuel cells in microgrids: Opportunities and challenges. *BMC Energy* **2019**, *1*, 1–23.
24. Ghenai, C.; Salameh, T.; Merabet, A. Design, optimization, and control of standalone solar PV/fuel cell hybrid power system. In Proceedings of the 2017 International Renewable and Sustainable Energy Conference (IRSEC), Tangier, Morocco, 4–7 December 2017; pp. 1–5.
25. Cao, Y.; Li, Y.; Zhang, G.; Jermsittiparsert, K.; Razmjooy, N. Experimental modeling of PEM fuel cells using a new improved seagull optimization algorithm. *Energy Rep.* **2019**, *5*, 1616–1625. [CrossRef]
26. Larminie, J.; Dicks, A.; McDonald, M.S. *Fuel Cell Systems Explained*; Wiley: Chichester, UK, 2003; Volume 2.
27. Mann, R.F.; Amphlett, J.C.; Hooper, M.A.; Jensen, H.M.; Peppley, B.A.; Roberge, P.R. Development and application of a generalized steady-state electrochemical model for a PEM fuel cell. *J. Power Sources* **2000**, *86*, 173–180. [CrossRef]
28. Hamrouni, N.; Chérif, A. Modelling and control of a grid connected photovoltaic system. *Rev. Energ. Renouvelables* **2007**, *10*, 335–344.
29. Idoniboyeobu, D.C.; Orike, S.; Biragbara, P.B. Optimization of a grid-connected photovoltaic system using fuzzy logic control. *Eur. J. Electr. Eng. Comput. Sci.* **2017**, *1*. Available online: https://ejece.org/index.php/ejece/article/view/7 (accessed on 25 April 2021). [CrossRef]